

000
001
002
003
004
005
006
007
008
009
010
011
012

Supplement for: **DeepCoDA: personalized interpretability for compositional health data**

013
014
015
016
017
018
019

0.1. Study 4: 2-levels of interpretability (expanded)

020
021
022
023
024
025
026
027
028

The **DeepCoDA** framework offers 2-levels of interpretability: (1) the "weights" of the self-explanation module (layer w in Figure 1 of the main paper) tell us how the classifier predicts a class label; (2) the weights of the log-bottleneck module (θ_z in Figure 1 of the main paper) tell us which features contribute to each log-contrast.

029
030
031
032
033
034
035
036

At the **first level**, the product scores ($w_i * z_i$) can be interpreted directly by a clinical laboratory or researcher to identify which features drive the final prediction. When a classifier makes a decision, the patient-specific weights (w_i) are multiplied with the log-contrast values (z_i), then added together. In data set "3", a patient is predicted to have inflammatory bowel disease if this sum exceeds zero; otherwise, the patient is healthy. The largest product scores contribute most to the decision.

037
038
039
040
041

Consider two patients, chosen randomly:

- Patient 26 is healthy: their product scores are [2.0, -15.6, -3.6, -1.1, 1.8].
- Patient 13 is unhealthy: their product scores are [0.5, -7.3, 8.8, 7.4, 0.1].

042
043
044
045
046
047

For patient 26, the second term is highly negative, suggesting that the patient is healthy. Since the second term is derived from the second log-contrast, we can infer that log-contrast 2 is most important for this prediction.

048
049
050
051
052
053
054

For patient 13, the third and fourth terms are highly positive, suggesting that the patient is unhealthy. Interestingly, the second is highly negative (like patient 26), suggesting that the second log-contrast "looks" healthy. However, this negative score is not enough to sway the final decision.

At the **second level**, the log-bottleneck weights define how each bacteria contribute to the ratios. For log-contrast 3, the bacteria *Gordonibacter pamelaee* makes the largest contribution to the numerator, while *Bacteroides cellulosilyticus* makes the largest contribution to the denominator. For patient 13, the log-contrast values are [0.61, -2.98, -4.64, 5.79, -1.76]. The signs of the log-contrasts reveal which

bacteria dominate. Negative values mean that the denominator bacteria outweigh those in the numerator; positives mean that the numerator outweighs the denominator.

Meanwhile, our canonical correlation analysis reminds us that the importance of log-contrast 3 (w_3) depends on the value of log-contrast 2 (z_2), via an interaction learned automatically from the data. The top panels in Figure 5 summarize the distribution of these patient-specific weights and log-contrast values across the entire patient cohort.

055
056
057
058
059
060
061
062
063
064
065
066
067
068
069
070
071
072
073
074
075
076
077
078
079
080
081
082
083
084
085
086
087
088
089
090
091
092
093
094
095
096
097
098
099
100
101
102
103
104
105
106
107
108
109

| Data set ID | # Samples | # Features | # Classes | Class 1 | Class 2 |
|-------------|-----------|------------|-----------|---------------------------|-----------------------|
| 1 | 975 | 48 | 2 | Crohn's disease | Without |
| 2 | 128 | 60 | 2 | Men who have sex with men | Without |
| 3 | 220 | 153 | 2 | Control | IBD |
| 4 | 164 | 158 | 2 | Crohn's disease | Ulcerative colitis |
| 5 | 220 | 885 | 2 | Control | IBD |
| 6 | 164 | 885 | 2 | Crohn's disease | Ulcerative colitis |
| 7 | 182 | 278 | 2 | Case | Diarrheal control |
| 8 | 247 | 610 | 2 | Case | Non-Diarrheal control |
| 9 | 292 | 1133 | 2 | Colorectal cancer (CRC) | Without |
| 10 | 318 | 1302 | 2 | Colorectal cancer (CRC) | Non-CRC control |
| 11 | 1182 | 188 | 2 | Primary solid tumor | Solid tissue normal |
| 12 | 1004 | 188 | 2 | Her2 Cancer | Not Her2 Cancer |
| 13 | 718 | 188 | 2 | LumA Cancer | LumB Cancer |
| 14 | 140 | 992 | 2 | Crohn's disease (ileum) | Without (ileum) |
| 15 | 160 | 992 | 2 | Crohn's disease (rectum) | Without (rectum) |
| 16 | 2070 | 3090 | 2 | GI tract | Oral |
| 17 | 180 | 3090 | 2 | Female | Male |
| 18 | 404 | 3090 | 2 | Stool | Tongue (dorsum) |
| 19 | 408 | 3090 | 2 | Subgingival plaque | Supragingival plaque |
| 20 | 172 | 980 | 2 | Healthy | Colorectal cancer |
| 21 | 124 | 2526 | 2 | Without | Diabetes |
| 22 | 130 | 2579 | 2 | Cirrhosis | Without |
| 23 | 199 | 660 | 2 | Black | Hispanic |
| 24 | 342 | 660 | 2 | Nugent score high | Nugent score low |
| 25 | 200 | 660 | 2 | Black | White |

Table 1. Characteristics of the 25 data sets used in Section 4.3.

110
111
112
113
114
115
116
117
118
119
120
121
122
123
124
125
126
127
128
129
130
131
132
133
134
135
136
137
138
139
140
141
142
143
144
145
146
147
148
149
150
151
152
153
154
155
156
157
158
159
160
161
162
163
164

| Data set ID | Original source | Retrieved via |
|--------------------|----------------------------------|--|
| 1 | doi: 10.1016/j.chom.2014.02.005 | doi: 10.1128/mSystems.00053-18 |
| 2 | doi: 10.1016/j.ebiom.2016.01.032 | doi: 10.1128/mSystems.00053-18 |
| 3 | doi: 10.1038/s41564-018-0306-4 | supplemental materials |
| 4 | doi: 10.1038/s41564-018-0306-4 | supplemental materials |
| 5 | doi: 10.1038/s41564-018-0306-4 | supplemental materials |
| 6 | doi: 10.1038/s41564-018-0306-4 | supplemental materials |
| 7 | doi: 10.1128/mBio.01021-14 | doi: doi.org/10.1038/s41467-017-01973-8 |
| 8 | doi: 10.1128/mBio.01021-15 | doi: doi.org/10.1038/s41467-017-01973-9 |
| 9 | doi: 10.1186/s13073-016-0290-3 | doi: doi.org/10.1038/s41467-017-01973-10 |
| 10 | doi: 10.1186/s13073-016-0290-3 | doi: doi.org/10.1038/s41467-017-01973-11 |
| 11 | doi: 10.1038/ng.2764 | labels from doi: 10.1186/s13058-016-0724-2 |
| 12 | doi: 10.1038/ng.2764 | labels from doi: 10.1186/s13058-016-0724-2 |
| 13 | doi: 10.1038/ng.2764 | labels from doi: 10.1186/s13058-016-0724-2 |
| 14 | doi: 10.1016/j.chom.2014.02.005 | doi: 10.1093/gigascience/giz042 |
| 15 | doi: 10.1016/j.chom.2014.02.005 | doi: 10.1093/gigascience/giz043 |
| 16 | doi: 10.1038/nature11209 | doi: 10.1093/gigascience/giz044 |
| 17 | doi: 10.1038/nature11209 | doi: 10.1093/gigascience/giz045 |
| 18 | doi: 10.1038/nature11209 | doi: 10.1093/gigascience/giz046 |
| 19 | doi: 10.1038/nature11209 | doi: 10.1093/gigascience/giz047 |
| 20 | doi: 10.1101/gr.126573.111 | doi: 10.1093/gigascience/giz048 |
| 21 | doi: 10.1038/nature11450 | doi: 10.1093/gigascience/giz049 |
| 22 | doi: 10.1038/nature13568 | doi: 10.1093/gigascience/giz050 |
| 23 | doi: 10.1073/pnas.1002611107 | doi: 10.1093/gigascience/giz051 |
| 24 | doi: 10.1073/pnas.1002611107 | doi: 10.1093/gigascience/giz052 |
| 25 | doi: 10.1073/pnas.1002611107 | doi: 10.1093/gigascience/giz053 |

Table 2. Sources for the 25 data sets used in Section 4.3.

165
166
167
168
169
170
171
172
173
174
175
176
177
178
179
180
181
182
183
184
185
186
187
188
189
190
191
192
193
194
195
196
197
198
199
200
201
202
203
204
205
206
207
208
209
210
211
212
213
214
215
216
217
218
219

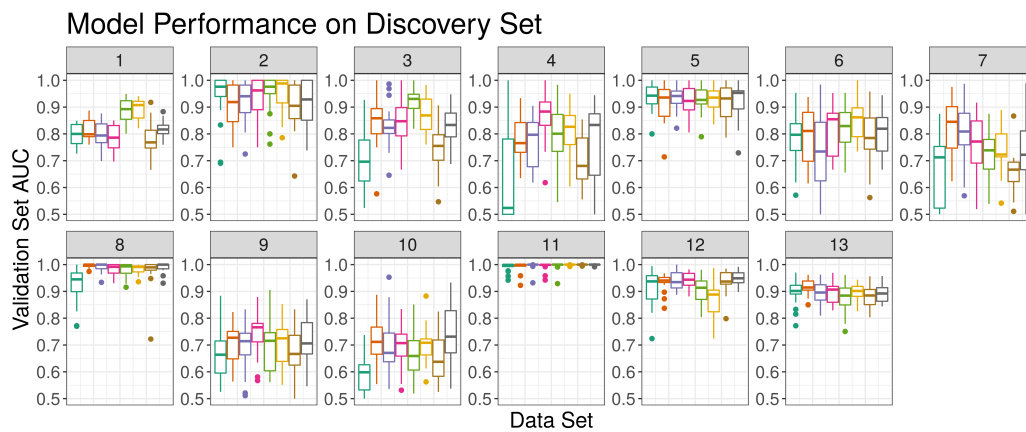


Figure 1. This figure shows the AUC for several models, organized by the method (x-axis) and data set source (facet). For all models, the boxplot shows the AUC distribution across 20 random 90%-10% training-test set splits. All **DeepCoDA** models use 5 log-bottlenecks and an L1 penalty of 0.01, chosen based on the “discovery set”. Our model achieves appreciable performance across the 25 data sets. However, our aim is not to improve performance, but to extend personalized interpretability to compositional data.

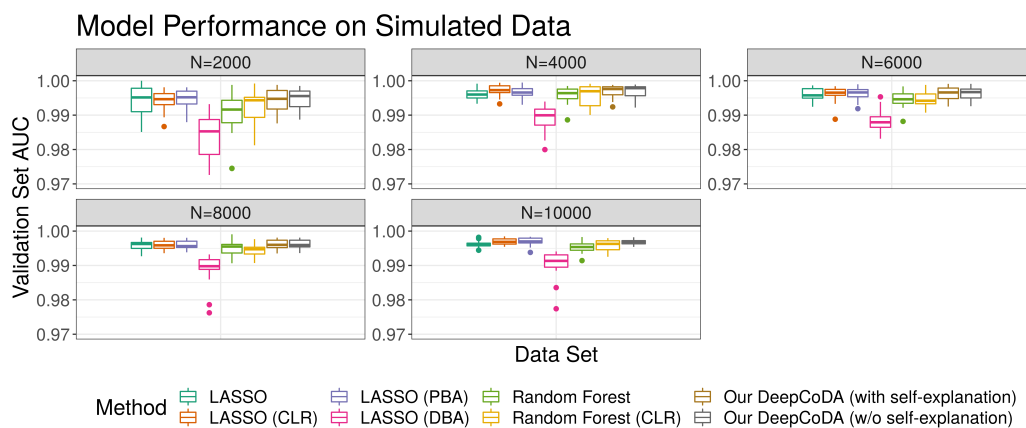


Figure 2. This figure shows the AUC for several models, organized by the method (x-axis) and number of samples in the second synthetic data set (facet). For all models, the boxplot shows the AUC distribution across 20 random 90%-10% training-test set splits. This figure confirms that the **DeepCoDA** model can scale to larger data sets with many samples.